

CMB statistical anisotropy from noncommutative gravitational waves

Maresuke Shiraishi,^{a,b} David F. Mota,^c Angelo Ricciardone^{a,b} and Frederico Arroja^b

^aDipartimento di Fisica e Astronomia “G. Galilei”, Università degli Studi di Padova, via Marzolo 8, I-35131, Padova, Italy

^bINFN, Sezione di Padova, via Marzolo 8, I-35131, Padova, Italy

^cInstitute of Theoretical Astrophysics, University of Oslo, P.O. Box 1029 Blindern, N-0315 Oslo, Norway

E-mail: maresuke.shiraishi@pd.infn.it, d.f.mota@astro.uio.no, angelo.ricciardone@pd.infn.it, arroja@pd.infn.it

Abstract. Primordial statistical anisotropy is a key indicator to investigate early Universe models and has been probed by the cosmic microwave background (CMB) anisotropies. In this paper, we examine tensor-mode CMB fluctuations generated from anisotropic gravitational waves, parametrised by $P_h(\mathbf{k}) = P_h^{(0)}(k)[1 + \sum_{LM} f_L(k)g_{LM}Y_{LM}(\hat{\mathbf{k}})]$, where $P_h^{(0)}(k)$ is the usual scale-invariant power spectrum. Such anisotropic tensor fluctuations may arise from an inflationary model with noncommutativity of fields. It is verified that in this model, an isotropic component and a quadrupole asymmetry with $f_0(k) = f_2(k) \propto k^{-2}$ are created and hence highly red-tilted off-diagonal components arise in the CMB power spectra, namely $\ell_2 = \ell_1 \pm 2$ in TT , TE , EE and BB , and $\ell_2 = \ell_1 \pm 1$ in TB and EB . We find that B-mode polarisation is more sensitive to such signals than temperature and E-mode polarisation due to the smallness of large-scale cosmic variance and we can potentially measure $g_{00} = 30$ and $g_{2M} = 58$ at 68% CL in a cosmic-variance-limited experiment. Such a level of signal may be measured in a PRISM like experiment, while the instrumental noise contaminates it in the *Planck* experiment. These results imply that it is impossible to measure the noncommutative parameter if it is small enough for the perturbative treatment to be valid. Our formalism and methodology for dealing with the CMB tensor statistical anisotropy are general and straightforwardly applicable to other early Universe models.

Contents

1	Introduction	1
2	Noncommutative gravitational waves	2
2.1	Noncommutative system	2
2.2	Quantization	3
2.3	Tensor power spectrum	4
3	Signatures in the CMB anisotropies	5
3.1	CMB power spectrum	5
3.2	Error estimation	6
4	Conclusion	9

1 Introduction

Noncommutativity in quantum fluctuations may be a key property of fundamental theories at ultra high energy scales, such as string theory and Lorentz-violating theories (see e.g., refs. [1–6]). These theories have been well-studied for the purpose of solving several open issues in cosmology and high energy physics such as magnetogenesis (e.g., refs. [7–11]).

Quantum fluctuations affected by noncommutativity in the very early Universe can imprint their characteristic signatures in cosmological observables. A space-time noncommutativity can induce primordial curvature perturbations, which breaks rotational and parity invariance [12–18]. These act as seeds of the cosmic microwave background (CMB) anisotropies and generate dipole or quadrupole anisotropy in the CMB power spectrum [13, 15, 17, 19, 20]. Nowadays, primordial noncommutativity has attracted attention from both purely theoretical and phenomenological sides.

In addition to the curvature perturbation, the noncommutativity also affects the tensor-mode sector, i.e, gravitational waves. In ref. [21], the impacts of tensor-mode noncommutativity on the present gravitational wave background (GWB) have been investigated. There, the authors have taken into account not the space-time noncommutativity but the noncommutativity of fields by the so-called noncommutative field approach. This is also motivated by the Lorentz-violating gravity [6, 22, 23]. The resulting GWB originates from the inflationary tensor-mode perturbations, while the superhorizon modes of such seed perturbations should also create CMB tensor-mode fluctuations at late times. The present paper examines such CMB signatures for the first time. We find that, in the same manner as the scalar-mode case, resultant CMB power spectra violate rotational invariance since the noncommutativity of fields induces a preferred direction.

Probing statistical anisotropy in the CMB fluctuations is one of the most interesting and attractive topics in cosmology (e.g., refs. [24–27]). Current CMB temperature data in the *Planck* experiment indicates nonzero dipole anisotropy [28] and also gives the most accurate bound on the quadrupole anisotropy [29]. These results have been obtained from the CMB scalar-mode power spectra. On the other hand, meaningful signals can also arise in the tensor-mode sector as shown in the present noncommutative case. In this sense, probing the statistical anisotropy from the tensor-mode power spectra should be a beneficial study. In

the present paper, we show how the tensor-mode statistical anisotropy can be measured in current and forthcoming experiments such as *Planck* [30] or PRISM [31, 32].

To analyse the CMB signatures, at first, we derive the power spectrum of the inflationary gravitational wave by following ref. [21]. Then, it is obvious that the noncommutativity produces the quadrupole anisotropy. We express its magnitude through the spherical harmonic coefficients, g_{LM} , given by

$$P_h(\mathbf{k}) = P_h^{(0)}(k) \left[1 + \sum_{L=0}^{\infty} \sum_{M=-L}^L f_L(k) g_{LM} Y_{LM}(\hat{\mathbf{k}}) \right], \quad (1.1)$$

where $P_h^{(0)}(k)$ is the usual scale-invariant isotropic power spectrum. This parametrisation is similar to the scalar-mode case [33]. In the present noncommutative case, g_{LM} vanishes except in $L = 0$ and 2 due to parity conservation. Interestingly, $f_0(k) = f_2(k) \propto k^{-2}$ is found, and hence we observe a highly red-tilted power spectrum of the CMB fluctuations. Applying the quadratic maximum likelihood (QML) estimator utilised in weak lensing analysis [34, 35], we compute the expected uncertainty on g_{LM} . Then, we perform joint analyses of the auto- and cross-spectra between temperature, E-mode and B-mode polarisations. As a consequence, we find that B-mode signals are more informative and can potentially measure $g_{00} = 30$ and $g_{2M} = 58$, where $M = 0, \pm 1, \pm 2$, at 68% CL.

The plan of this paper is as follows. In the next section, we derive the power spectrum of the inflationary gravitational waves. In section 3, we compute the resulting CMB power spectra and evaluate the expected uncertainty on g_{LM} by using the QML estimator. The final section is devoted to the conclusion.

2 Noncommutative gravitational waves

In this section, we estimate the power spectrum of inflationary gravitational waves under the presence of noncommutativity of fields. The model we discuss here has been firstly analysed by ref. [21] for the purpose of the GWB measurement. Here, we shall compute the superhorizon-scale power spectrum of primordial gravitational waves, which creates tensor-mode power spectra of the CMB fluctuations in the late-time Universe.

2.1 Noncommutative system

Let us consider gravitational waves, \bar{h}_{ij} , on the FLRW background, namely $ds^2 = a^2(\tau)[-d\tau^2 + (\delta_{ij} + \bar{h}_{ij})dx^i dx^j]$, where $a(\tau)$ is the scale factor as a function of conformal time τ and $\partial_i \bar{h}_{ij} = \bar{h}_{ii} = 0$. We start from the standard quadratic action in the tensor-mode sector:

$$\begin{aligned} S &= \frac{M_{\text{pl}}^2}{8} \int d\tau d^3x a^2 \left[\dot{\bar{h}}_{ij}^2 - (\partial_l \bar{h}_{ij})^2 \right] \\ &= \frac{1}{4} \int d\tau d^3x \left[\dot{h}_{ij}^2 + \frac{\ddot{a}}{a} h_{ij}^2 - (\partial_l h_{ij})^2 \right], \end{aligned} \quad (2.1)$$

where $\dot{} \equiv \partial_\tau$ denotes a derivative with respect to conformal time and $M_{\text{pl}} = 1/\sqrt{8\pi G}$ is the reduced Planck mass. To derive the second equality, we have introduced canonical

normalisation $h_{ij} \equiv aM_{\text{pl}}\bar{h}_{ij}/\sqrt{2}$. Then, we impose the noncommutativity of fields as¹

$$\begin{aligned} [h_{\mathbf{k}}^{(\lambda)}(\tau), h_{\mathbf{k}'}^{(\lambda')}(\tau)] &= 0, \\ [h_{\mathbf{k}}^{(\lambda)}(\tau), p_{\mathbf{k}'}^{(\lambda')}(\tau)] &= \frac{i}{2}(2\pi)^3\delta^{(3)}(\mathbf{k} + \mathbf{k}')\delta_{\lambda,\lambda'}, \\ [p_{\mathbf{k}}^{(\lambda)}(\tau), p_{\mathbf{k}'}^{(\lambda')}(\tau)] &= -\lambda\boldsymbol{\alpha} \cdot \hat{\mathbf{k}}(2\pi)^3\delta^{(3)}(\mathbf{k} + \mathbf{k}')\delta_{\lambda,\lambda'}, \end{aligned} \quad (2.2)$$

where $h_{\mathbf{k}}^{(\lambda)}$ and $p_{\mathbf{k}}^{(\lambda)} \equiv \frac{1}{2}\dot{h}_{\mathbf{k}}^{(\lambda)}$ denote the $\lambda = \pm 2$ helicity-space expressions of the gravitational wave h_{ij} and its conjugate momentum $p_{ij} = \delta\mathcal{L}/\delta\dot{h}_{ij} = \frac{1}{2}\dot{h}_{ij}$ with \mathcal{L} being the Lagrangian density of the corresponding action, and h_{ij} is given by

$$h_{ij}(\mathbf{x}, \tau) = \int \frac{d^3\mathbf{k}}{(2\pi)^3} \sum_{\lambda=\pm 2} h_{\mathbf{k}}^{(\lambda)}(\tau) e_{ij}^{(\lambda)}(\hat{\mathbf{k}}) e^{i\mathbf{k}\cdot\mathbf{x}}. \quad (2.3)$$

The polarisation tensor $e_{ij}^{(\lambda)}(\hat{\mathbf{k}})$ satisfies $e_{ii}^{(\lambda)}(\hat{\mathbf{k}}) = \hat{k}_i e_{ij}^{(\lambda)}(\hat{\mathbf{k}}) = 0$ (transverse and traceless condition), $e_{ij}^{(\lambda)}(\hat{\mathbf{k}}) e_{ij}^{(\lambda')}(\hat{\mathbf{k}}) = 2\delta_{\lambda,-\lambda'}$ (normalisation) and $e_{ij}^{(\lambda)*}(\hat{\mathbf{k}}) = e_{ij}^{(-\lambda)}(\hat{\mathbf{k}}) = e_{ij}^{(\lambda)}(-\hat{\mathbf{k}})$ [36]. The so-called noncommutative parameter $\boldsymbol{\alpha}$ expresses the size and the direction of the noncommutativity of the conjugate momenta. Notice that the usual commutative relations are restored by $\boldsymbol{\alpha} = 0$. Physically, the magnitude of $\boldsymbol{\alpha}$ determines the comoving energy scale where the noncommutativity plays a significant role in graviton propagation. In the following discussions, for simplicity, let us analyze the phenomenological signatures of the noncommutativity in a special case: $\boldsymbol{\alpha} = \text{const}$, although it may be possible to consider running $\boldsymbol{\alpha}$.

2.2 Quantization

The present case imposes the noncommutativity between conjugate momenta (2.2). This noncommutative effect may be interpreted as an additional term breaking the Lorentz invariance in an effective action [21]:

$$S^{\text{new}} \equiv \frac{1}{4} \int d\tau d^3x \left[\dot{h}_{ij}^2 + \frac{\ddot{a}}{a} h_{ij}^2 - (\partial_l h_{ij})^2 - 8\alpha_m \eta_{jkm} h_{kl} \dot{h}_{lj} \right], \quad (2.4)$$

with η_{ijk} being the three dimensional antisymmetric tensor normalised as $\eta_{123} = 1$, and the usual commutation relations are restored, reading

$$\begin{aligned} [h_{\mathbf{k}}^{(\lambda)}(\tau), \pi_{\mathbf{k}'}^{(\lambda')}(\tau)] &= \frac{i}{2}(2\pi)^3\delta^{(3)}(\mathbf{k} + \mathbf{k}')\delta_{\lambda,\lambda'}, \\ [\pi_{\mathbf{k}}^{(\lambda)}(\tau), \pi_{\mathbf{k}'}^{(\lambda')}(\tau)] &= 0. \end{aligned} \quad (2.5)$$

Here, the helicity-state expression of the new conjugate momentum $\pi_{ij} \equiv \delta\mathcal{L}^{\text{new}}/\delta\dot{h}_{ij}$ is given by $\pi_{\mathbf{k}}^{(\lambda)} = \frac{1}{2}e_{ij}^{(-\lambda)}(\hat{\mathbf{k}})\pi_{ij}(\mathbf{k}) = p_{\mathbf{k}}^{(\lambda)} - i\lambda\boldsymbol{\alpha} \cdot \hat{\mathbf{k}}h_{\mathbf{k}}^{(\lambda)}$. This process is the so-called noncommutative field approach and, owing to eq. (2.5), we can perform the normal quantization process as described below.

¹Here, we use the helicity-state representations, instead of usual Fourier-space ones, e.g., $[h_{ij}(\mathbf{k}, \tau), p_{kl}(\mathbf{k}', \tau)]$, seen in the original paper [21], because the expressions are simpler and the transverse and traceless conditions are automatically satisfied.

Quantized gravitational waves can be expressed as

$$h_{\mathbf{k}}^{(\lambda)}(\tau) = v_{\mathbf{k}}^{(\lambda)}(\tau)\beta(\mathbf{k}, \lambda) + v_{-\mathbf{k}}^{(\lambda)*}(\tau)\beta^\dagger(-\mathbf{k}, \lambda) , \quad (2.6)$$

where $\hat{\mathbf{k}}$ denotes a unit vector and the creation β^\dagger and annihilation β operators obey $\beta(\mathbf{k}, \lambda)|0\rangle = 0$ and $[\beta(\mathbf{k}, \lambda), \beta^\dagger(\mathbf{k}', \lambda')] = (2\pi)^3 \delta_{\lambda, \lambda'} \delta^{(3)}(\mathbf{k} - \mathbf{k}')$, with $\lambda, \lambda' = \pm 2$. Using these relations, one can understand that the above commutation relations (2.2) and (2.5) equate to the conditions on the mode function $v_{\mathbf{k}}^{(\lambda)}$:

$$\begin{aligned} |v_{\mathbf{k}}^{(\lambda)}|^2 &= |v_{-\mathbf{k}}^{(\lambda)}|^2 , \\ v_{\mathbf{k}}^{(\lambda)} \dot{v}_{\mathbf{k}}^{(\lambda)*} - v_{-\mathbf{k}}^{(\lambda)*} \dot{v}_{-\mathbf{k}}^{(\lambda)} &= i , \\ |\dot{v}_{\mathbf{k}}^{(\lambda)}|^2 - |\dot{v}_{-\mathbf{k}}^{(\lambda)}|^2 &= -4\lambda \boldsymbol{\alpha} \cdot \hat{\mathbf{k}} . \end{aligned} \quad (2.7)$$

These will be used to determine the normalisation of the mode functions.

2.3 Tensor power spectrum

The variation of the action (2.4) with respect to $h_{\mathbf{k}}^{(\lambda)}$ leads to the equation of motion:

$$\ddot{v}_{\mathbf{k}}^{(\lambda)} - 4i\lambda \boldsymbol{\alpha} \cdot \hat{\mathbf{k}} \dot{v}_{\mathbf{k}}^{(\lambda)} + \left(k^2 - \frac{\ddot{a}}{a}\right) v_{\mathbf{k}}^{(\lambda)} = 0 , \quad (2.8)$$

where we have used an useful relation: $\eta_{ijk} e_{il}^{(\lambda)}(\hat{\mathbf{k}}) e_{jl}^{(\lambda')}(\hat{\mathbf{k}}) = -i\lambda \hat{k}_k \delta_{\lambda, -\lambda'}$ [36]. Note that this form is valid in terms of any direction of $\boldsymbol{\alpha}$ and coincides with the result in ref. [21] under the condition where $\boldsymbol{\alpha}$ is parallel to the z axis.

Let us work in standard slow-roll inflation, namely

$$\frac{\ddot{a}}{a} \simeq \frac{\nu^2 - \frac{1}{4}}{\tau^2} , \quad (2.9)$$

where $\nu = \frac{3}{2} + \frac{\epsilon}{1-\epsilon}$ with ϵ being the slow-roll parameter. Then, by imposing eq. (2.7) as initial conditions on subhorizon scales, we can easily find a solution of eq. (2.8) as

$$v_{\mathbf{k}}^{(\lambda)}(\tau) = \frac{\sqrt{\pi}}{2} e^{i(\frac{\nu\pi}{2} + \frac{\pi}{4})} \sqrt{-\tau} e^{2i\lambda \boldsymbol{\alpha} \cdot \hat{\mathbf{k}} \tau} H_\nu^{(1)}(-l\tau) , \quad (2.10)$$

where $H_\nu^{(1)}(x)$ is the Hankel function of the first kind and $l \equiv \sqrt{k^2 + 16(\boldsymbol{\alpha} \cdot \hat{\mathbf{k}})^2}$. One can see from this form that the presence of the noncommutativity changes the phase and the dispersion relation of the mode function. The power spectrum of the original gravitational waves \bar{h}_{ij} is straightforwardly given by

$$\left\langle \prod_{i=1}^2 \bar{h}_{\mathbf{k}_i}^{(\lambda_i)}(\tau) \right\rangle = (2\pi)^3 \frac{P_h(\mathbf{k}_1, \tau)}{2} \delta_{\lambda_1, \lambda_2} \delta^{(3)}(\mathbf{k}_1 + \mathbf{k}_2) , \quad (2.11)$$

$$P_h(\mathbf{k}, \tau) = \frac{4}{a^2 M_{\text{pl}}^2} |v_{\mathbf{k}}^{(\lambda)}(\tau)|^2 . \quad (2.12)$$

Assuming de-Sitter like space-time ($\epsilon \approx 0$ or $\nu \approx \frac{3}{2}$), the superhorizon power spectrum which acts as a source of the CMB power spectra becomes

$$P_h(\mathbf{k}) \approx \frac{2H^2}{M_{\text{pl}}^2} l^{-3} \approx \frac{2H^2}{M_{\text{pl}}^2} k^{-3} \left[1 - 24(\hat{\boldsymbol{\alpha}} \cdot \hat{\mathbf{k}})^2 \left(\frac{\alpha}{k}\right)^2 \right] , \quad (2.13)$$

where H is the Hubble parameter. In the final approximation, we have treated the anisotropic part perturbatively. Together with the positiveness of the power spectrum, this restricts the values of the noncommutative parameter one can analyze to $|\boldsymbol{\alpha} \cdot \hat{\mathbf{k}}| \ll k/5$. The observational limit on the anisotropy of the scalar fluctuations suggests that this is a reasonable assumption also for the tensor mode [27, 29].

Interestingly, this form involves the quadrupole anisotropy depending on k^{-5} . It is a consequence of the quadratic dependence of l on $\boldsymbol{\alpha} \cdot \hat{\mathbf{k}}$. Accordingly, the resulting CMB power spectra break the statistical isotropy and off-diagonal signals, namely $\ell_1 \neq \ell_2$, will arise. Note that parity invariance is kept since spin- λ dependence cancels out.

3 Signatures in the CMB anisotropies

In this section, we shall discuss signatures of the anisotropic gravitational waves in the CMB temperature and polarisation power spectra, and we investigate the expected uncertainty on the magnitude of anisotropy from observations using the quadratic maximum-likelihood (QML) estimator [34, 35].

For convenience of analysis, let us express the anisotropic power spectrum of gravitational waves by the spherical harmonic expansion (1.1), where $P_h^{(0)}(k) = \frac{2H^2}{M_{\text{pl}}^2} k^{-3} = \frac{r}{2} \frac{2\pi^2}{k^3} A_S$ is the isotropic part of the tensor power spectrum parametrised by the tensor-to-scalar ratio r and the amplitude of scalar fluctuations ($A_S = 2.23 \times 10^{-9}$ [37]). In the present noncommutative scenario, the anisotropic coefficient becomes

$$g_{LM} = -16 \left(\frac{\alpha}{k_0} \right)^2 \left[\sqrt{\pi} \delta_{L,0} \delta_{M,0} + \frac{4\pi}{5} Y_{LM}^*(\hat{\boldsymbol{\alpha}}) \delta_{L,2} \right], \quad (3.1)$$

where $g_{LM}^* = (-1)^M g_{L-M}$ holds and we have set $f_0(k) = f_2(k) = (k/k_0)^{-2}$ with $1/k_0 = \tau_0 = 14$ Gpc being the present horizon scale. In subsection 3.2, we estimate the expected error bar on g_{LM} instead of $\boldsymbol{\alpha}$. Then, note that g_{00} is sensitive to the size of noncommutativity $\alpha = |\boldsymbol{\alpha}|$ alone, while the direction of noncommutativity $\hat{\boldsymbol{\alpha}}$ is only determined by the g_{2M} measurement.

We notice that this form is appropriate under the perturbative treatment of the anisotropic part and the positiveness of the power spectrum for any direction of $\boldsymbol{\alpha}$, i.e., $\alpha \ll k/5$. With the projection $\ell \sim k\tau_0$, the corresponding CMB scale is roughly evaluated as $\ell \gg 5\alpha/k_0$. This means that the CMB computation based on eq. (2.13) is valid for $\alpha/k_0 \ll 2/5$, since the largest CMB scale is $\ell = 2$. This condition is also compatible with a bound evaluated from a constraint on today's graviton mass, namely $\alpha \lesssim 0.01 \text{ Mpc}^{-1}$ [21].

3.1 CMB power spectrum

The tensor-mode CMB anisotropy is expressed as [36, 38]

$$a_{\ell m}^X = 4\pi(-i)^\ell \int \frac{d^3\mathbf{k}}{(2\pi)^3} \mathcal{T}_\ell^X(k) \sum_{\lambda=\pm 2} \left(\frac{\lambda}{2} \right)^x \bar{h}_{\mathbf{k}}^{(\lambda)}{}_{-\lambda} Y_{\ell m}^*(\hat{\mathbf{k}}), \quad (3.2)$$

where $X = T$ (temperature), E (E-mode polarisation) and B (B-mode polarisation), $\lambda = \pm 2$ denotes the spin of the tensor mode and x represents the parity of the field, namely $x = 0$ for $X = T, E$ and $x = 1$ for $X = B$. $\mathcal{T}_\ell^X(k)$ is the radiation transfer function and expresses the enhancements of the temperature mode for $\ell \lesssim 100$ due to the integrated Sachs-Wolfe

effect and two peaks at $\ell \sim 10$ and 100 in the polarisation modes due to Thomson scattering. We assume that anisotropic effects of the noncommutativity on the transfer function are negligible. Taking the ensemble average of the square of $a_{\ell m}^X$ and dealing with the addition of angular momentum as shown in ref. [36], the CMB power spectrum is formulated as

$$\langle a_{\ell_1 m_1}^{X_1} a_{\ell_2 m_2}^{X_2*} \rangle = C_{\ell_1 \ell_2}^{X_1 X_2}(\gamma = 0) \delta_{x_1, x_2} \delta_{\ell_1, \ell_2} \delta_{m_1, m_2} + \sum_{L=0,2} C_{\ell_1 m_1 \ell_2 m_2}^{X_1 X_2}(L), \quad (3.3)$$

where the anisotropic power spectrum is

$$C_{\ell_1 m_1 \ell_2 m_2}^{X_1 X_2}(L) = i^{\ell_2 - \ell_1} C_{\ell_1 \ell_2}^{X_1 X_2}(\gamma = -2) \delta_{x_1 + x_2 + \ell_1 + \ell_2}^{\text{even}} I_{\ell_1 \ell_2 L}^{-220} \times \sum_M g_{LM} (-1)^{m_1} \begin{pmatrix} \ell_1 & \ell_2 & L \\ -m_1 & m_2 & M \end{pmatrix}, \quad (3.4)$$

with

$$C_{\ell_1 \ell_2}^{X_1 X_2}(\gamma) \equiv \frac{2}{\pi} \int_0^\infty k^2 dk \mathcal{T}_{\ell_1}^{X_1}(k) \mathcal{T}_{\ell_2}^{X_2}(k) P_h^{(0)}(k) \left(\frac{k}{k_0} \right)^\gamma, \quad (3.5)$$

$$I_{\ell_1 \ell_2 L}^{s_1 s_2 s_3} \equiv \sqrt{\frac{(2\ell_1 + 1)(2\ell_2 + 1)(2\ell_3 + 1)}{4\pi}} \begin{pmatrix} \ell_1 & \ell_2 & \ell_3 \\ s_1 & s_2 & s_3 \end{pmatrix}, \quad (3.6)$$

$$\delta_l^{\text{even}} \equiv \begin{cases} 1 & (l = \text{even}) \\ 0 & (l = \text{odd}) \end{cases}. \quad (3.7)$$

The anisotropic power spectrum satisfies $C_{\ell_1 m_1 \ell_2 m_2}^{X_1 X_2*}(L) = (-1)^{m_1 + m_2} C_{\ell_1 - m_1 \ell_2 - m_2}^{X_1 X_2}(L)$ and $C_{\ell_1 m_1 \ell_2 m_2}^{X_1 X_2}(L) = C_{\ell_2 m_2 \ell_1 m_1}^{X_2 X_1*}(L)$. The selection rules in $\delta_{x_1 + x_2 + \ell_1 + \ell_2}^{\text{even}}$ and $I_{\ell_1 \ell_2 L}^{-220}$ allow nonzero TT , TE , EE and BB in $\ell_2 = \ell_1$ and $\ell_1 \pm 2$, and TB and EB in $\ell_2 = \ell_1 \pm 1$. We can also notice that TB and EB vanish when $L = 0$ because rotational invariance, namely $\delta_{\ell_1, \ell_2} \delta_{m_1, m_2}$, is kept. These are common signatures of the primordial quadrupole anisotropy in the CMB power spectra [39, 40].

Figure 1 depicts auto- and cross-correlated power spectra of the temperature and polarisations generated from the quadrupole anisotropy: $C_{\ell_1 m_1 \ell_2 m_2}^{X_1 X_2}(L = 2)$ for $m_1 = m_2 = 1$. Here, the direction of α is fixed to be parallel to the z axis and hence $Y_{LM}(\hat{\alpha}) = \sqrt{\frac{2L+1}{4\pi}} \delta_{M,0}$ holds. In this figure, it is obvious that compared with the usual scale-invariant case, the CMB power spectra have highly red-tilted shapes due to the additional k^{-2} dependence of the quadrupole anisotropy. One may also notice that the two parity-odd correlations (TB and EB) decay more rapidly than the other four parity-even ones. Due to this scale dependence, the expected error on g_{LM} converges at very low ℓ as shown in the next subsection.

3.2 Error estimation

As in the present noncommutative case, when the statistical anisotropy in the CMB power spectrum is regarded as a tiny modulation of the scale-invariant isotropic component, it can be well-estimated by using the QML estimator [34, 35]. Then, the Fisher matrix for g_{LM} can be written as

$$\mathcal{F}_{LM, L'M'} = \sum_{i,j} \frac{\delta \mathbf{C}^i(L)}{\delta g_{LM}^*} (\mathbf{Cov}^{-1})^{ij} \left(\frac{\delta \mathbf{C}^j(L')}{\delta g_{L'M'}^*} \right)^*, \quad (3.8)$$

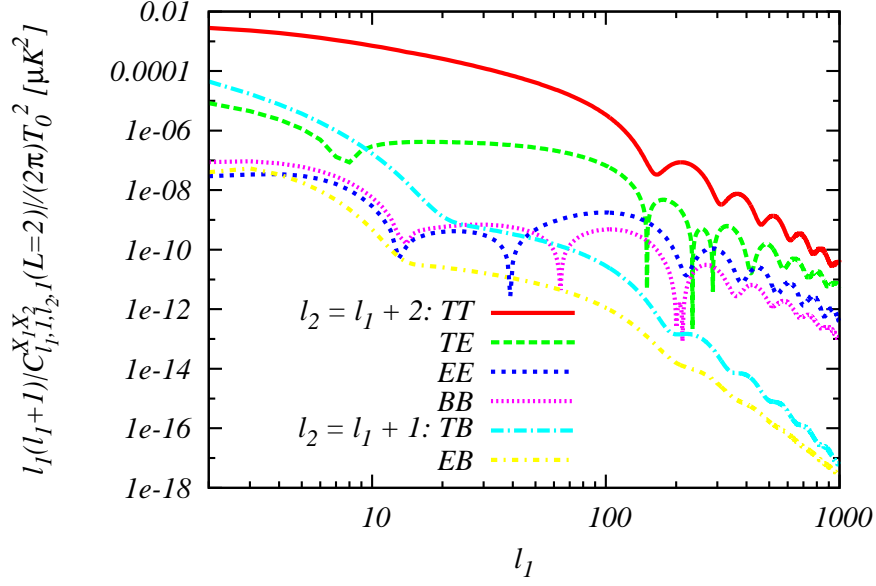


Figure 1. CMB quadrupole power spectrum: $C_{\ell_1, \ell_2}^{X_1 X_2}(L=2)$ for $\ell_2 = \ell_1 + 2$ (TT , TE , EE and BB) and $\ell_2 = \ell_1 + 1$ (TB and EB). Here, we set $r = 10^{-2}$ and $\alpha/k_0 = 0.1$, and fix α to be along z axis. Then, $g_{2M} \approx -0.25\delta_{M,0}$ holds.

where i and j runs over given sets of auto- and cross-correlated power spectra, \mathbf{C}^i is the i th CMB power spectrum and \mathbf{Cov}^{ij} is the covariance matrix element given by the i th and j th power spectra. For simplicity, let us ignore off-diagonal elements in the observed power spectra, i.e., $\langle a_{\ell_1 m_1}^{\text{obs}} a_{\ell_2 m_2}^{\text{obs}*} \rangle \approx \tilde{C}_{\ell_1, \ell_2} \delta_{m_1, m_2}$. Furthermore, on the basis of the fact that $C_{\ell_1 \ell_2}^{X_1 X_2}(\gamma) \approx C_{\ell_1 \ell_2}^{X_2 X_1}(\gamma)$ for $\ell_2 - 2 \leq \ell_1 \leq \ell_2 + 2$, we can obtain that $C_{\ell_1 m_1 \ell_2 m_2}^{X_1 X_2}(L) \approx (-1)^{m_1 + m_2} C_{\ell_2 - m_2 \ell_1 - m_1}^{X_1 X_2}(L)$. After these two approximations the Fisher matrix is reduced to

$$\begin{aligned}
\mathcal{F}_{LM, L'M'} &\approx \sum_{\ell_1 m_1 \ell_2 m_2} \sum_{\substack{i \leftrightarrow X_1 X_2 \\ j \leftrightarrow X'_1 X'_2}} \frac{\delta C_{\ell_1 m_1 \ell_2 m_2}^i(L)}{\delta g_{LM}^*} (\text{Cov}^{-1})_{\ell_1 \ell_2}^{ij} \left(\frac{\delta C_{\ell_1 m_1 \ell_2 m_2}^j(L')}{\delta g_{L'M'}^*} \right)^* \\
&= \sum_{\ell_1 \ell_2} \sum_{\substack{i \leftrightarrow X_1 X_2 \\ j \leftrightarrow X'_1 X'_2}} \delta_{x'_1 + x'_2 + \ell_1 + \ell_2}^{\text{even}} \delta_{x_1 + x_2 + \ell_1 + \ell_2}^{\text{even}} (I_{\ell_1 \ell_2}^{-220})^2 \frac{\delta_{LL'} \delta_{MM'}}{2L + 1} \\
&\quad \times C_{\ell_1 \ell_2}^i(\gamma = -2) (\text{Cov}^{-1})_{\ell_1 \ell_2}^{ij} C_{\ell_1 \ell_2}^j(\gamma = -2), \tag{3.9}
\end{aligned}$$

with

$$\text{Cov}_{\ell_1 \ell_2}^{ij} = \tilde{C}_{\{\ell_1\}}^{X_1 X'_1} \tilde{C}_{\{\ell_2\}}^{X_2 X'_2} + \tilde{C}_{\{\ell_1\}}^{X_1 X'_2} \tilde{C}_{\{\ell_2\}}^{X_2 X'_1}, \tag{3.10}$$

where $A_{\{\ell_1\} B_{\ell_2\}} \equiv \frac{1}{2}[A_{\ell_1} B_{\ell_2} + A_{\ell_2} B_{\ell_1}]$ denotes the symmetrization under the permutation of ℓ_1 and ℓ_2 .

From now, we consider error estimations from three auto-correlations (TT , EE and BB), a combination of the temperature and E-mode anisotropies ($TT + TE + EE$) and a

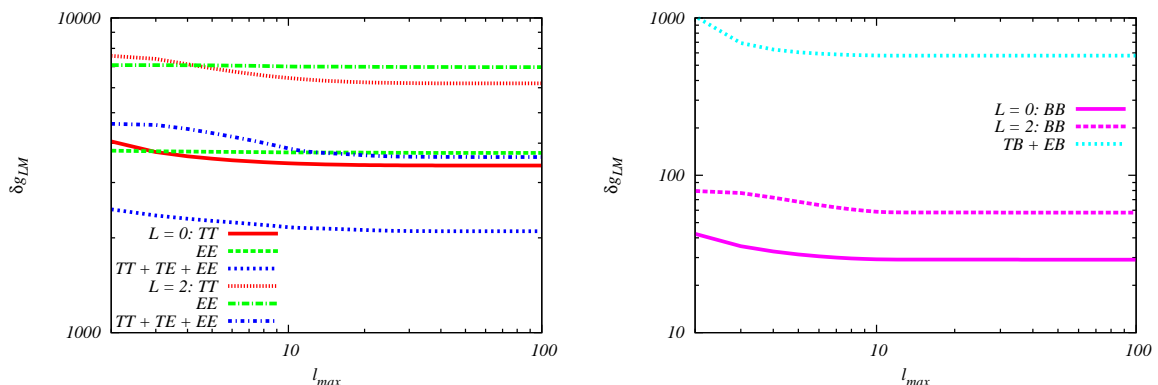


Figure 2. δg_{00} and δg_{2M} estimated from TT , EE , $TT + TE + EE$ (left panel), BB and $TB + EB$ (right panel) in a cosmic-variance-limited experiment. Here, we take $r = 10^{-2}$.

parity-odd combination ($TB + EB$). The covariance matrix involves the observed power spectrum \tilde{C}_ℓ that is the sum of the signal and the instrumental noise. In this paper, let us consider the noise information of the *Planck* and the proposed PRISM experiments [30, 31, 41]. As the temperature and E-mode signals, we adopt the CMB power spectra consistent with the *Planck* data [37]. On the other hand, the observed B-mode spectrum is still unknown and here we simply assume that the B-mode signal is consistent with the scale-invariant isotropic power spectrum $C_{\ell\ell}^{BB}(\gamma = 0)$. Recall that this magnitude is proportional to the tensor-to-scalar ratio r . Moreover, for simplicity, we adopt a null hypothesis for the observed TB and EB correlations, i.e., $\tilde{C}_\ell^{TB} = \tilde{C}_\ell^{EB} = 0$.

Figure 2 describes the numerical results of 1σ errors on g_{LM} given by

$$\delta g_{LM} = \mathcal{F}_{LM,LM}^{-1/2}. \quad (3.11)$$

δg_{LM} does not depend on M because in the analysis we ignore the off-diagonal elements in the covariance matrix. In figure 2, we assume a cosmic-variance-limited experiment. One can observe from this figure that δg_{LM} converges before $\ell_{\max} \sim 100$ owing to the highly red-tilted CMB spectra as shown in figure 1. It is obvious that when $r = 10^{-2}$, δg_{LM} exceeds 10^3 in the analysis with the temperature or E-mode polarisation, while the analysis with the B-mode polarisation reduces δg_{LM} by one or two orders of magnitude. This is a consequence that the cosmic variances in the temperature and E-mode polarisation are much larger than the B-mode cosmic variance with $r = 10^{-2}$. In the measurements of the temperature and E-mode polarisation, because the theoretical power spectrum $C_{\ell_1\ell_2}^{X_1X_2}(\gamma)$ is proportional to r and there is no r dependence in the covariance matrix, a simple scaling relation $\delta g_{LM}^{TT} \propto \delta g_{LM}^{EE} \propto \delta g_{LM}^{TT+TE+EE} \propto r^{-1}$ holds. Meanwhile, if involving the B-mode information, the covariance matrix also depends on r . Especially, in a cosmic-variance-limited experiment, the covariance matrix is determined by r alone, and hence we obtain $\delta g_{LM}^{BB} \propto r^0$ and $\delta g_{LM}^{TB+EB} \propto r^{-1/2}$ (see also table 1). The results in figure 2 and these magnitude relations lead to the conclusion that, for $r < 10^{-2}$, namely r allowed by current observations, the most stringent constraint on g_{LM} comes from BB . We can also notice a rough relation $\delta g_{2M} \sim 2\delta g_{00}$ in all cases.

Table 1 presents δg_{LM} estimated from the B-mode polarisation (BB and $TB + EB$) under the *Planck*, PRISM and ideal cosmic-variance-limited experiments. We take $r = 10^{-2}$ and 10^{-4} for comparison. This table shows that the *Planck* measurement cannot detect g_{LM}

r	BB		$TB + EB$	
	10^{-2}	10^{-4}	10^{-2}	10^{-4}
<i>Planck</i>	180 (87)	9100 (4600)	1200	92000
PRISM	73 (36)	160 (78)	700	11000
ideal	58 (30)	58 (30)	580	5800

Table 1. δg_{2M} (and δg_{00}) estimated from BB and $TB + EB$ assuming $r = 10^{-2}$ and 10^{-4} . Here, we take into account the effect of 70% sky coverage ($f_{\text{sky}} = 0.7$) in the *Planck* and PRISM cases by following $\delta g_{LM} \propto f_{\text{sky}}^{-1/2}$. Note that we only describe δg_{2M} in the $TB + EB$ analysis because of the absence of $L = 0$ signals. In the ideal experiment, δg_{LM} from $TB + EB$ is exactly proportional to $r^{-1/2}$, while for BB it is independent of r .

less than $\mathcal{O}(10 - 100)$ except in the BB analysis with $r = 10^{-2}$. In contrast, the BB analysis by the PRISM experiment will measure it at 68 % CL even if r is very small (e.g., $r = 10^{-4}$). In case that r is large, $TB + EB$ may also become a good observable.

The range of α coming from our perturbative treatment (2.13), namely $\alpha/k_0 \ll 2/5$, corresponds to g_{LM} satisfying $|g_{LM}| \lesssim \mathcal{O}(1)$. The above results indicate that such small α cannot be measured.

4 Conclusion

Noncommutativity is a key indicator of non-standard high energy physics and it may imprint interesting effects on the primordial fluctuations. This paper has focused on signatures of primordial gravitational waves affected by the noncommutativity of fields in the observed CMB fluctuations.

In addition to the usual isotropic (nearly) scale-invariant power spectrum of gravitational waves, the noncommutativity gives two contributions with k^{-5} dependence: an isotropic and a quadrupolar ones. Hence, the resulting CMB power spectra are highly red-tilted and have non-vanishing off-diagonal components, i.e., $\ell_2 = \ell_1 \pm 2$ in TT , TE , EE and BB , and $\ell_2 = \ell_1 \pm 1$ in TB and EB .

By applying the QML estimator, we have estimated the expected uncertainty on the statistical anisotropy. We have used the usual spherical harmonic parametrisation with coefficients g_{LM} and computed the 1σ error bars δg_{LM} through the analyses of auto-correlations, i.e., TT , EE and BB , and combined analyses with auto- and cross-correlations, i.e., $TT + TE + EE$ and $TB + EB$. Then, we have found that δg_{LM} converges before $\ell \sim 100$ because of the highly red-tilted spectrum shapes. We have confirmed that, since the B-mode cosmic variance is much smaller than the temperature and E-mode ones on such large scales, BB is most informative to measure g_{LM} . Potentially, we can measure $g_{00} = 30$ and $g_{2M} = 58$, where $M = 0, \pm 1, \pm 2$, at 68% CL in a cosmic-variance-limited experiment. It is hard to measure g_{LM} with *Planck* due to the lack of sensitivity to polarisations, while a PRISM like experiment may attain such accuracy level.

Our analysis has showed that if the noncommutative parameter α is enough small for the perturbative treatment to be justified, it is impossible to detect it even in the ideal noise-free experiment. On the other hand, there may exist theoretical models predicting detectable tensor g_{LM} . The formalism and methodology for dealing with the CMB statistical anisotropy developed in the present paper will be applicable to future phenomenological studies on such models.

Acknowledgments

We thank Michele Liguori for useful comments. MS was supported in part by a Grant-in-Aid for JSPS Research under Grant No. 25-573. DFM thanks Research Council of Norway. This work was partly supported in part by the ASI/INAF Agreement I/072/09/0 for the Planck LFI Activity of Phase E2.

References

- [1] N. Seiberg and E. Witten, *String theory and noncommutative geometry*, *JHEP* **9909** (1999) 032, [[hep-th/9908142](#)].
- [2] N. Seiberg, L. Susskind, and N. Toumbas, *Space-time noncommutativity and causality*, *JHEP* **0006** (2000) 044, [[hep-th/0005015](#)].
- [3] D. F. Mota, M. Sandstad, and T. Zlosnik, *Cosmology of the selfaccelerating third order Galileon*, *JHEP* **1012** (2010) 051, [[arXiv:1009.6151](#)].
- [4] D. A. Easson, R. Gregory, D. F. Mota, G. Tasinato, and I. Zavala, *Spinflation*, *JCAP* **0802** (2008) 010, [[arXiv:0709.2666](#)].
- [5] S. Tsujikawa, R. Maartens, and R. Brandenberger, *Noncommutative inflation and the CMB*, *Phys.Lett.* **B574** (2003) 141–148, [[astro-ph/0308169](#)].
- [6] A. Ferrari, M. Gomes, J. Nascimento, E. Passos, A. Y. Petrov, *et. al.*, *Lorentz violation in the linearized gravity*, *Phys.Lett.* **B652** (2007) 174–180, [[hep-th/0609222](#)].
- [7] A. Mazumdar and M. M. Sheikh-Jabbari, *Noncommutativity in space and primordial magnetic field*, *Phys.Rev.Lett.* **87** (2001) 011301, [[hep-ph/0012363](#)].
- [8] B. Li, D. Fonseca Mota, and J. D. Barrow, *Detecting a Lorentz-Violating Field in Cosmology*, *Phys.Rev.* **D77** (2008) 024032, [[arXiv:0709.4581](#)].
- [9] J. Gamboa and J. Lopez-Sarrion, *U(1) noncommutative gauge fields and magnetogenesis*, *Phys.Rev.* **D71** (2005) 067702, [[hep-th/0501034](#)].
- [10] A. P. Kouretsis, *Cosmic magnetization in curved and Lorentz violating space-times*, [[arXiv:1312.4631](#)].
- [11] O. Bertolami and D. Mota, *Primordial magnetic fields via spontaneous breaking of Lorentz invariance*, *Phys.Lett.* **B455** (1999) 96–103, [[gr-qc/9811087](#)].
- [12] S. Alexander, R. Brandenberger, and J. Magueijo, *Noncommutative inflation*, *Phys.Rev.* **D67** (2003) 081301, [[hep-th/0108190](#)].
- [13] F. Lizzi, G. Mangano, G. Miele, and M. Peloso, *Cosmological perturbations and short distance physics from noncommutative geometry*, *JHEP* **0206** (2002) 049, [[hep-th/0203099](#)].
- [14] S. Koh and R. H. Brandenberger, *Cosmological perturbations in non-commutative inflation*, *JCAP* **0706** (2007) 021, [[hep-th/0702217](#)].
- [15] E. Akofer, A. Balachandran, S. Jo, A. Joseph, and B. Qureshi, *Direction-Dependent CMB Power Spectrum and Statistical Anisotropy from Noncommutative Geometry*, *JHEP* **0805** (2008) 092, [[arXiv:0710.5897](#)].
- [16] A. Kobakhidze, *Imprints of microcausality violation on the cosmic microwave background*, [[arXiv:0811.0242](#)].
- [17] T. S. Koivisto and D. F. Mota, *CMB statistics in noncommutative inflation*, *JHEP* **1102** (2011) 061, [[arXiv:1011.2126](#)].
- [18] A. Nautiyal, *Anisotropic non-gaussianity with noncommutative spacetime*, *Physics Letters* **B728** (2014) 472–481, [[arXiv:1303.4159](#)].

- [19] E. Akofor, A. Balachandran, A. Joseph, L. Pekowsky, and B. A. Qureshi, *Constraints from CMB on Spacetime Noncommutativity and Causality Violation*, *Phys.Rev.* **D79** (2009) 063004, [[arXiv:0806.2458](#)].
- [20] K. Karwan, *CMB constraints on noncommutative geometry during inflation*, *Eur.Phys.J.* **C69** (2010) 521–529, [[arXiv:0903.2806](#)].
- [21] Y.-f. Cai and Y.-S. Piao, *Probing noncommutativity with inflationary gravitational waves*, *Phys.Lett.* **B657** (2007) 1–9, [[gr-qc/0701114](#)].
- [22] J. Carmona, J. Cortes, J. Gamboa, and F. Mendez, *Noncommutativity in field space and Lorentz invariance violation*, *Phys.Lett.* **B565** (2003) 222–228, [[hep-th/0207158](#)].
- [23] H. Falomir, J. Gamboa, J. Lopez-Sarrion, F. Mendez, and A. da Silva, *Vortices, infrared effects and Lorentz invariance violation*, *Phys.Lett.* **B632** (2006) 740–744, [[hep-th/0504032](#)].
- [24] N. Groeneboom, H. Eriksen, K. Gorski, G. Huey, J. Jewell, *et. al.*, *Bayesian analysis of white noise levels in the 5-year WMAP data*, *Astrophys.J.* **702** (2009) L87–L90, [[arXiv:0904.2554](#)].
- [25] M. J. Axelsson, F. K. Hansen, T. Koivisto, and D. F. Mota, *CMB Anomalies from Imperfect Dark Energy: Confrontation with the Data*, [arXiv:1109.2778](#).
- [26] N. Groeneboom, M. Axelsson, D. Mota, and T. Koivisto, *Imprints of a hemispherical power asymmetry in the seven-year WMAP data due to non-commutativity of space-time*, [arXiv:1011.5353](#).
- [27] S. R. Ramazanov and G. Rubtsov, *Constraining anisotropic models of early Universe with WMAP9 data*, [arXiv:1311.3272](#).
- [28] **Planck Collaboration** Collaboration, P. Ade *et. al.*, *Planck 2013 results. XXIII. Isotropy and statistics of the CMB*, [arXiv:1303.5083](#).
- [29] J. Kim and E. Komatsu, *Limits on anisotropic inflation from the Planck data*, *Phys.Rev.* **D88** (2013) 101301, [[arXiv:1310.1605](#)].
- [30] **Planck Collaboration** Collaboration, P. Ade *et. al.*, *Planck 2013 results. I. Overview of products and scientific results*, [arXiv:1303.5062](#).
- [31] **PRISM Collaboration** Collaboration, P. Andre *et. al.*, *PRISM (Polarized Radiation Imaging and Spectroscopy Mission): A White Paper on the Ultimate Polarimetric Spectro-Imaging of the Microwave and Far-Infrared Sky*, [arXiv:1306.2259](#).
- [32] P. Andre, C. Baccigalupi, A. Banday, D. Barbosa, B. Barreiro, *et. al.*, *The Polarized Radiation Imaging and Spectroscopy Mission*, [arXiv:1310.1554](#).
- [33] A. R. Pullen and M. Kamionkowski, *Cosmic Microwave Background Statistics for a Direction-Dependent Primordial Power Spectrum*, *Phys.Rev.* **D76** (2007) 103529, [[arXiv:0709.1144](#)].
- [34] D. Hanson and A. Lewis, *Estimators for CMB Statistical Anisotropy*, *Phys.Rev.* **D80** (2009) 063004, [[arXiv:0908.0963](#)].
- [35] D. Hanson, A. Lewis, and A. Challinor, *Asymmetric Beams and CMB Statistical Anisotropy*, *Phys.Rev.* **D81** (2010) 103003, [[arXiv:1003.0198](#)].
- [36] M. Shiraishi, D. Nitta, S. Yokoyama, K. Ichiki, and K. Takahashi, *CMB Bispectrum from Primordial Scalar, Vector and Tensor non-Gaussianities*, *Prog.Theor.Phys.* **125** (2011) 795–813, [[arXiv:1012.1079](#)].
- [37] **Planck Collaboration** Collaboration, P. Ade *et. al.*, *Planck 2013 results. XVI. Cosmological parameters*, [arXiv:1303.5076](#).
- [38] M. Shiraishi, S. Yokoyama, D. Nitta, K. Ichiki, and K. Takahashi, *Analytic formulae of the CMB bispectra generated from non-Gaussianity in the tensor and vector perturbations*, *Phys.Rev.* **D82** (2010) 103505, [[arXiv:1003.2096](#)].

- [39] M.-a. Watanabe, S. Kanno, and J. Soda, *Imprints of Anisotropic Inflation on the Cosmic Microwave Background*, *Mon.Not.Roy.Astron.Soc.* **412** (2011) L83–L87, [[arXiv:1011.3604](#)].
- [40] J. Soda, *Statistical Anisotropy from Anisotropic Inflation*, *Class.Quant.Grav.* **29** (2012) 083001, [[arXiv:1201.6434](#)].
- [41] M. Shiraishi, *Polarization bispectrum for measuring primordial magnetic fields*, *JCAP* **1311** (2013) 006, [[arXiv:1308.2531](#)].